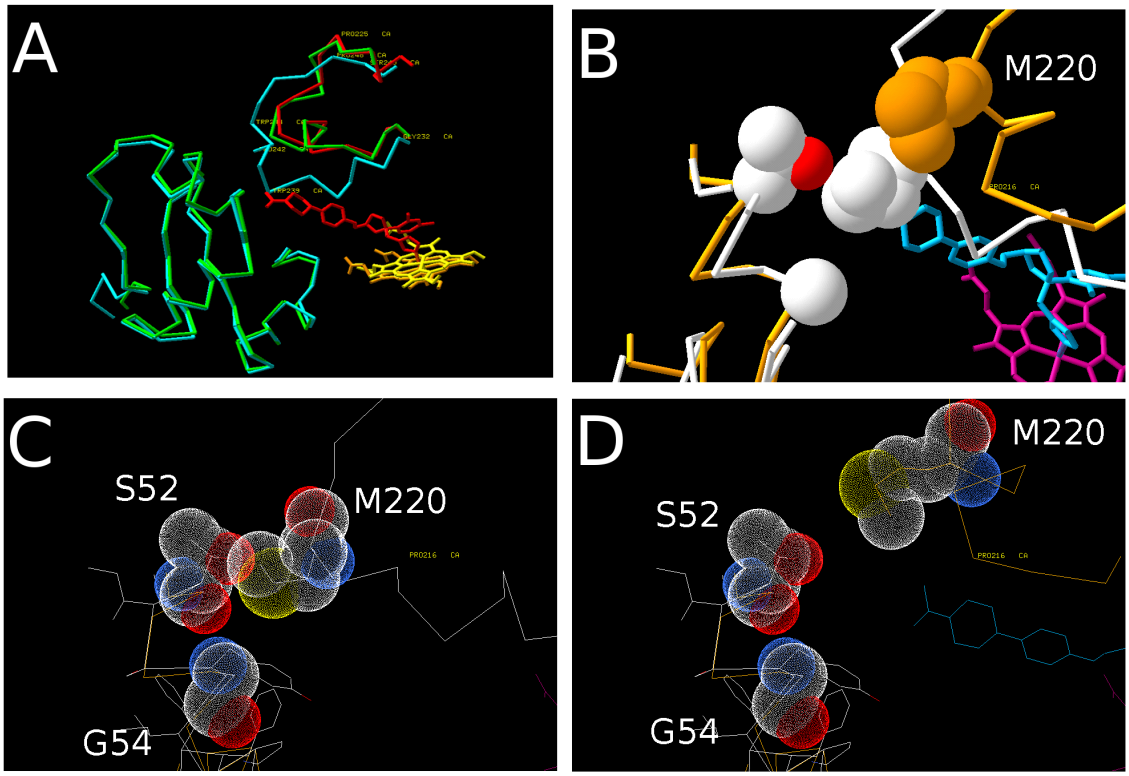

Supplementary Figure 1. Comparison of model structures based on azole bound (3JUS) and unbound (3LD6) templates. **A**; Superposition of Af293 CYP51A structures for the active site cleft based on azole bound 3JUS template (green CA trace) and unbound 3LD6 template (blue CA trace). Minor difference in the A1163 structure derived from 3JUS are shown (red CA trace). Heme and azole positions are relatively unchanged in the two structures (**A**) and residues outside the entrance to the active site cleft have the same conformation in both structures (not shown). **B**, **C** and **D**; Spacefill models of structures in **A** showing possible interaction between M220 and S52. Structure based on the 3JUS template is shown with an orange backbone and structure based on the 3LD6 template is shown with a white backbone. In the absence of azole M220 and S52 are juxtaposed © and may form an electrostatic bond. When azole is bound these residues are seperated (**D**). The predicted ketoconazole coordinates (blue) suggest stearic interation between M220 and the azole that may prevent M220-S52 interaction (**B**).

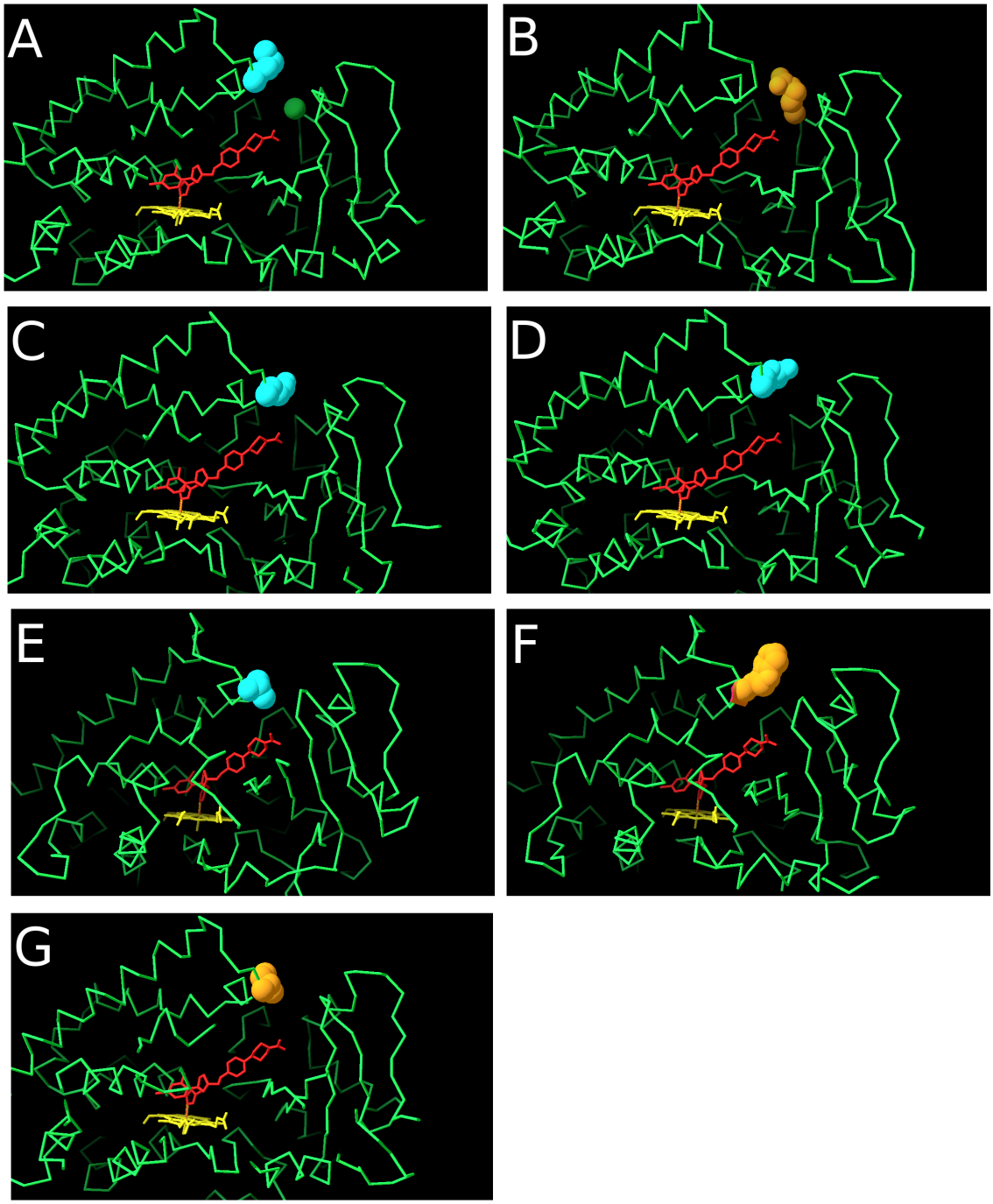

Supplementary figure 3. Common azole resistant mutations in the Af293 CYP51A gene. A; 30A slab showing the active site cleft of the predicted wild-type Af293 CYP51A structure. CA backbone is shown in green, heme in yellow, inferred ketoconazole position in red, M220 in blue and G54 in green; B; Predicted G54R mutation; C; M220K; D, M220R; E, M220V; F, M220W; G, M220I.